1 Introduction

Were the succession of stars endless, then the background of the sky would present us a uniform luminosity, like that displayed by the Galaxy -since there could be absolutely no point, in all that background, at which would not exist a star. The only mode, therefore, in which, under such a state of affairs, we could comprehend the voids which our telescopes find in innumerable directions, would be by supposing the distance of the invisible background so immense that no ray from it has yet been able to reach us at all.

Edgar Allen Poe on Olbers Paradox, Eureka (1848)

1.1 A Cosmopolitan Universe, life in the slow lane

The Universe is filled with a complex – bubble like – network consisting of voids, walls, filaments and clusters. This network connects neighbouring nodes of mass concentrations and separates large empty bubbles. In many respects it behaves and looks similar to human built (infra)structures (see Figure 1). The average to large cities would correspond to *Galaxies* and *Cluster of Galaxies* in the Universe. Such towns are located in the middle of a infrastructural web of electricity lines, highways and railways etc. The complexity of this network is often described by hierarchy of scales. A typical example is the road network, small roads branch of from larger highways that form the interconnections between large cities to average sized towns. The even smaller roads further link up to yet smaller villages. This cellular pattern of roads shows large holes that are outlined by large highways, they surround and separate more empty regions.

In the Universes the equivalent infrastructure of roads is called the Cosmic Web. It is made up of small filaments, walls, and larger filamentary bridges. Small filaments of dwarf galaxies connects average sized galaxies, and these are again part of larger filaments that bridge the clusters and superclusters into one connected superstructure. The dynamics in urban settlements are driven by social-economical forces set up mainly by differences in available job opportunities, status and wealth. The main force that drives the dynamics of the Cosmic Web is gravity.

In some sense normal galaxies can be considered as the average middle sized town. Such towns may merge and form larger cities that would correspond to clusters of galaxies. Larger cities conglomerate along rivers and coastal areas, forming larger urban areas. Notable examples of such extended metropolitan areas are the Randstad, Ruhr Gebiet, US East Coast etc.

Figure 1.1– Cosmopolitan light: When observing cities by night we are immediately struck by the largest and most luminous buildings. See for example the three characteristic horizon dominating spikes in the Figure above. These could correspond to the dense clusters in the Large scale structure. The latter is shown in projection on the sky. For such objects we have a relatively good understanding what makes them tick. But what about the light from less dense regions? In this work we shall describe the Cosmic Web from the perspective of the least dense regions. Within the analogy it corresponds to the light stemming from the more mundane situation shown in the lower foreground. It should be associated with the smaller peaks that reside in the darkest patches of the Cosmic Sky. Image courtesy of Rense Boomsma and EP.

The cosmic equivalents of these urban areas are the superclusters. These are clustered areas of clusters. In Figure 2 we show the Coma Great Wall, one of the most striking and well known superclusters in the nearby Universe.

Opposite to this densely populated urban environment is the remote and desolate outback. In such regions life is commonly less hectic and revolves at a slower pace. Toward the most desolate areas we may even find pristine land that for the most part has been left alone. In the Universe such underdense regions exist as well. In fact most of the Universe is filled up with these rather empty regions called voids. The name derives from the abbreviation of 'a region devoid of galaxies'.

In this thesis we will focus on the voids in the Universe. We will propose a way how to find the outlines of the voids. This provides us with a unique perspective on the overdense Cosmic Web. It allows us to address questions about the properties voids. For example what is the relation of the void with the overdense structures on its boundary? Is there an optimal way to reconstruct the density field that defines the voids, walls, filaments and clusters? What does the observed network of voids and large clusters in the real Universe look like? Do these structures behave in concordance with present day cosmological models? What are the

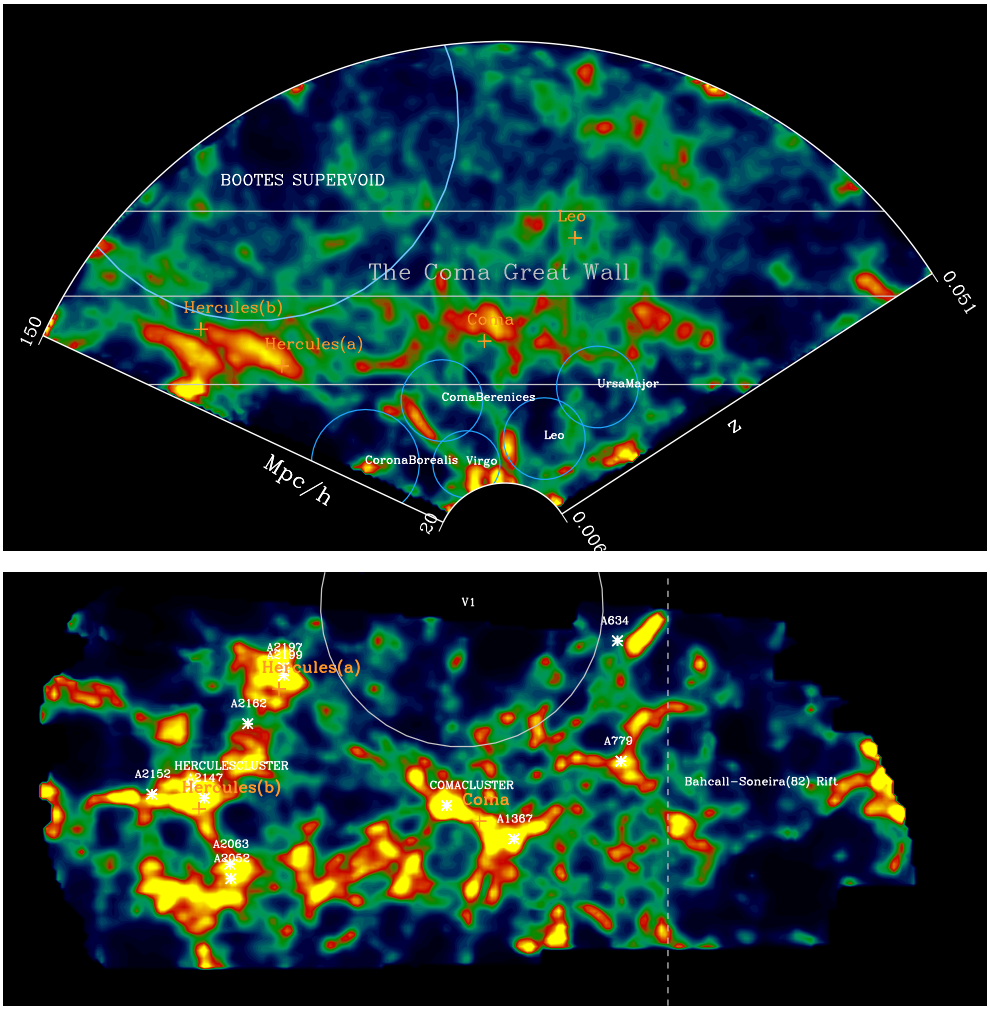

Figure 1.2– The Coma Great Wall: the figure shows the the Coma Great Wall. The top panel shows the density field as projected from the top. Some of the known nearby voids including their names are shown in the panel. We have indicated the most relevant superclusters and the Boötes Supervoid. A face-on projection (xz-projection) of the Coma Great Wall is shown in the lower figure. The superclusters and clusters are indicated in the figure. See Chapter 6 for an extensive analysis.

statistical properties of low density and high density regions? Are there consequences for galaxies that reside in voids?

1.2 Large Scale Structure Formation

In the most common accepted view of structure formation, galaxies, clusters and voids emerged from tiny primordial quantum fluctuations. These fluctuations rapidly expanded in size dur-

ing a period called inflation. After inflation these fluctuations were stretched out to very large scales. When these fluctuations entered again into the scale of the observable Universe gravitational growth could set in. The growth of these perturbations eventually formed the present day observable structures.

The evolution of this growth has a strong dependence on the contents of the Universe. The most important constituents of the Universe are baryons, radiation, dark matter and dark energy density. The densities are often specified in terms of a critical density ρ_c. At the critical density the Universe is spatially flat. Currently the favourite model is the concordance model or ΛCDM model (CDM= cold dark matter), with the following values;

$$\Omega_b = \frac{\rho_b}{\rho_c} = 0.0456, \quad \Omega_r = \frac{\rho_r}{\rho_c} = 0.005, \quad \Omega_d = \frac{\rho_d}{\rho_c} = 0.228, \quad \text{and} \quad \Omega_\Lambda = \frac{\Lambda}{3H^2} = 0.726, \tag{1.1}$$

The values are based on the 5th year data release of WMAP (Komatsu et al. 2009). The values of these fractional densities determines the global dynamics of the Universe. For our purposes here the dynamics of the Universe can be considered as a uniform expanding background, fully contained in the cosmological scale factor $a(t)$.

1.2.1 Gravitational Instability

The fluctuation field is described in terms of a density contrast field, $\delta(\mathbf{x})$.

$$\delta(\mathbf{x}) = \frac{\rho(\mathbf{x}) - \rho_m}{\rho_m}, \tag{1.2}$$

where ρ_m is the average density of the dark matter plus baryon density. It provides a framework to describe the fluctuations in the density field. Neglecting the pressure terms, the evolution of this gravitating pressureless fluid (dust) in an expanding background is given by

$$\frac{\partial \delta}{\partial t} + \frac{1}{a}\nabla \cdot [(1+\delta)\mathbf{v}] = 0\,, \tag{1.3}$$

$$\frac{\partial}{\partial t}(a\mathbf{v}) + (\mathbf{v}\cdot\nabla)\mathbf{v} = -\frac{\partial \phi}{\partial \mathbf{x}}\,, \tag{1.4}$$

$$\nabla^2\Phi = 4\pi G\rho_0 a^2 \delta\,. \tag{1.5}$$

The first two are the continuity equation and the Euler equation that describe the conservation of mass and momentum. The last is the Poisson equation that provides the solution for the gravitational potential field.

When the fluctuations and streaming motions are small the above equations can be linearised

$$\frac{\partial \delta^2}{\partial^2 t} + 2\frac{\dot{a}}{a}\frac{\partial \delta}{\partial t} = 4\pi G\rho_m \delta. \tag{1.6}$$

A solution to this equation is provided by

$$\delta(\mathbf{x}, t) = D(a)\, \delta_0(\mathbf{x}, t_0) \tag{1.7}$$

Here $D(a)$ is a universal linear growth factor that depends on the background cosmology. This background is again determined by the relative fractions of equation 1.1. For a flat and matter dominated universe $\Omega_m = \Omega_b + \Omega_d = 1$ the growth factor goes as $D(a) \propto a$, i.e. proportional to the expansion rate. In a low density matter dominated Universe $\Omega_m < 1$ the growth is smaller and is characterised by a freeze out time at $a_f = \frac{1-\Omega_m}{\Omega_m}$. After this freeze-out moment further

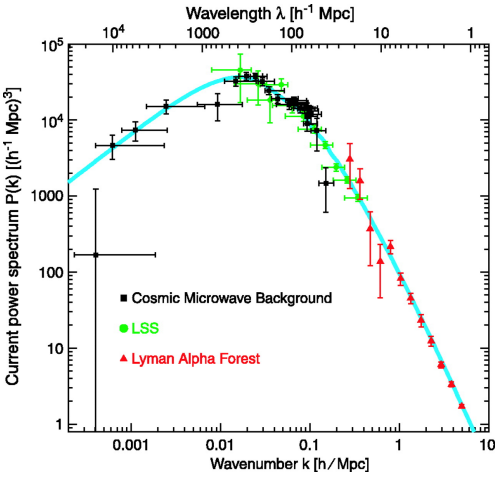

Figure 1.3– Power Spectrum: The figure shows the power spectrum estimated from a compilation of cosmological probes. The ΛCDM spectrum is shown for comparison. From Tegmark et al. (2004).

growth of structures stops. Also in ΛCDM model growth of structures is halted when the Universe starts to accelerate. This happens approximately at

$$a_{m\Lambda} = \left(\frac{2\Omega_\Lambda}{\Omega_m}\right)^{1/3} \tag{1.8}$$

1.2.2 Initial Fluctuations

Most observations suggest that the initial fluctuation field, generated in the early Universe, is well described by Gaussian random field. The one-point Probability Distribution Function of this Gaussian random field is given by

$$P_1(\delta)d\delta = \frac{1}{\sqrt{2\pi\sigma^2}} \exp\left(\frac{-\delta^2}{2\sigma^2}\right) d\delta \tag{1.9}$$

This is the probability for a small volume element having a density contrast value in the range of $(\delta, \delta + d\delta)$. The value of $\sigma \equiv \langle\delta^2\rangle$ is the variance of the density field. Since the Gaussian distribution is symmetric the skewness is $\langle\delta^3\rangle = 0$. For the initial density field it is assumed that the perturbations started out as small fluctuations, i.e. $\sigma \ll 1$. The first effect of linear structure growth ($\delta \propto D\delta_0$) will be to increase the variance of the field.

Besides the one-point distribution there are higher N-point distributions that describe the combined probabilities of the density values at more then one location. For a Gaussian Random fields the field is fully describe by the 2-point correlation function, ξ. It characterises the probability distribution of two points in the field having density value $\delta(\mathbf{x_1}) = \delta_1$ and $\delta(\mathbf{x_2}) = \delta_2$. The distribution belonging it is called the two-point density distribution. For a Gaussian Random Field it is given by

$$P_2(\delta_1, \delta_2) = \frac{1}{2\pi\sqrt{||\langle\delta_i\delta_j\rangle||}} \exp\left(-\frac{1}{2}\begin{pmatrix}\delta_1\\ \delta_2\end{pmatrix}\langle\delta_i\delta_j\rangle^{-1}(\delta_1\ \delta_2)\right) d\delta_1\delta_2 \tag{1.10}$$

Each of the $\delta_i = \delta(\mathbf{x_i})$ can be the density value anywhere in the spatial field. The matrix $\langle\delta_i\delta_j\rangle$ is the covariance matrix, with $||\langle\delta_i\delta_j\rangle||$ being the determinant of the matrix. The entries of this matrix are the auto-correlation Function

$$\langle\delta_1\delta_2\rangle = \xi(\mathbf{x_1} - \mathbf{x_2}) \tag{1.11}$$

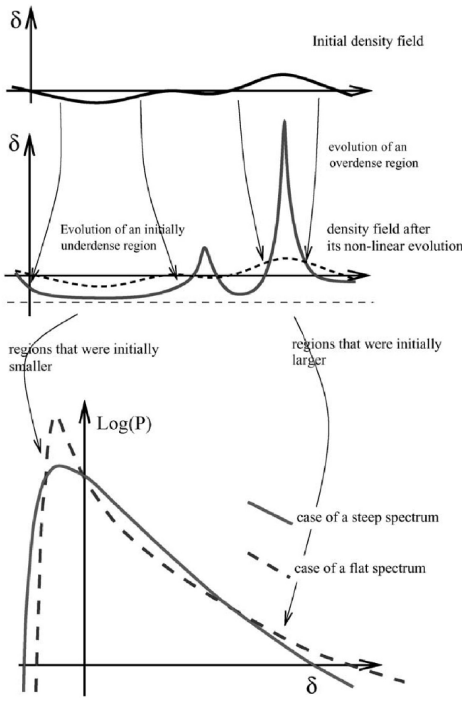

Figure 1.4– Nonlinear PDF the figure provides an animation of how the growth of structures influence the density distribution. This PDF will becomes skewed as nonlinear due to the collapse and growth of structures. From Bernardeau et al. (2002)

The correlation function is a function of distance, $\xi(r)$. It has a related function in the Fourier domain, called the Power Spectrum, $P(k)$. The spectrum provides the power at each particular scale, and thereby provides a means to show which scales are most relevant. The spectrum is often expressed in terms the spatial wave-numbers k, these wave-numbers are inversely proportional to scale or wavelength. Figure 1.3 shows an example of a combination of three measured power spectra, the power spectrum from the current favourite cosmological model (ΛCDM see eq.(1.1)) is also plotted.

Structure Growth

Small perturbations in a gravitational (pressureless) fluid are unstable. For example, if a region has a density that is only slightly higher than the average density. Here the potential field is lower and the gravitational force is directed inward. The region will start to contract, this will further increase the density, which increases the gravitational force, etc. Eventually the region collapses under its own gravitational influence, and becomes a virialized object.

If, on the other hand, the density was slightly lower than the mean density, we will get the opposite behaviour. Like overdense perturbations, also underdense perturbations are unstable. Here the initial gravitational force is directed outward. The region will therefore further expand and become more underdense. In turn this increases the gravitational force, the initial underdense region will further expand and eventually develop into a full dynamical object called a void.

This growth process has a consequence for the initial Gaussian distribution. Collapsed objects have a small volume and are of high density. This will create a long tail to high density values in the density distribution. The collapse of the peaks goes along with the outflow of

material from less dense regions. These underdense will fill up most of the volume, and this is reflected in the PDF as a pronounced peak at low density. The gravitational growth will make the density distribution less Gaussian and more asymmetric. As a consequence the skewness $\langle\delta^3\rangle$ and other higher moments will start to depart from zero. Figure 1.4 shows a graphical representation of this process. A further analysis of the present day PDF is presented in Chapter 7.

Non-Gaussian Conditions

Although the primordial density field seems to have been remarkably close to Gaussian, there are some indications to small but significant non-Gaussianties. Such non-Gaussianties may have originated during inflation, and may there provide a unique probe on the physics of the Early Universe. A well known parametrisation model of non-gaussianities are quadratic perturbations to the gravitational potential. Such distortions would show up in the density distribution as an amplification of the underdense or overdense tails in the distribution (see Grossi et al. 2008; Lam & Sheth 2009).

Higher order Moments

For the initial Gaussian density field the higher order moments are zero. Deviations from Gaussianity reveal themselves as nonzero higher order moments. The moments are relatively easily measurable, moreover their values can be calculated in the quasi-nonlinear growth regime (Peebles 1980; Juszkiewicz et al. 1993; Lokas et al. 1995). The quasi non-linear regime is distinct from the linear growth regime, because the variance is no longer $\langle\delta^2\rangle \ll 1$. Yet, the variance is still $\langle\delta^2\rangle \approx 1$ within this regime one can still make rather accurate predictions using perturbation theory. This makes it is distinct from the full non-linear growth where $\langle\delta^2\rangle > 1$.

The skewness $\langle\delta^3\rangle$ and kurtosis $\langle\delta^4\rangle$ are the higher order moments that have received most attention. In particular the normalised skewness S_3 and normalised kurtosis S_4.

$$S_3 = \frac{\langle\delta^3\rangle}{\langle\delta^2\rangle^2} = \frac{\bar{\xi}_3(V)}{\bar{\xi}_2(V)^2} \tag{1.12}$$

$$S_4 = \frac{\langle\delta^4\rangle - 3\sigma^4}{\langle\delta^2\rangle^4} = \frac{\bar{\xi}_4(V)}{\bar{\xi}_2(V)^3} \tag{1.13}$$

$$\tag{1.14}$$

In the quasi non-linear regime these normalised coefficients are almost independent of scale. There is a slight dependence on scale via the slope of the power spectrum, see Figure 1.4. They are more dependent on the level of biasing (see below) in the density field Fry & Gaztanaga (1993). Different higher order moments respond differently to the amount of biasing, therefore the higher order moments are more relevant for estimating the amount of biasing.

1.2.3 Galaxy Biasing

Galaxies are associated with peaks in the dark matter field. These peaks can be biased tracers, called 'peak-bias' (Kaiser 1984; Bardeen et al. 1986). This picture is further complicated by the fact the galaxy formation is a highly non-linear process, where various feedback mechanisms are involved. A peak or subhalo of a given mass may then harbour different kind of galaxies depending on its complete gastrophysical history. To model this accurately all the physical processes have to be take into account.

The relation between the dark matter field δ_d and the galaxy density field δ_g is simply called *biasing*. This term includes various different biasing schemes and definitions with a

varying degree of complexity. In its simplest form there is a deterministic relation between both fields. When such a direct relation exists, we may model it with a *biasing function*

$$\delta_g \equiv f(\delta_d) \equiv b(\delta_d)\delta_d. \tag{1.15}$$

The simplest proposed function is a linear relation. Here there is one constant b, called the bias parameter, representing the ratio between both fields. Given the fact that galaxy formation is such an involved nonlinear process, the validity of such a simple relationship would seem to be highly unlikely. As are result various generalisations of this model were proposed. These may involve stochastic, nonlinear, scale dependent and or time dependent components (see Pen 1998; Tegmark & Peebles 1998; Dekel & Lahav 1999; Matsubara 1999). In Chapter 7 we shall give a more detailed analysis about biasing.

1.2.4 Hierarchical Evolution

For cold dark matter the power spectrum has a particular interesting shape. The scale can be converted to a mass scale ($M \propto k^{-3}$). The fluctuation amplitude $\sigma(M)$ on the mass scale M is in the order of

$$\sigma(M)^2 \approx M^{-\frac{n+3}{3}} \tag{1.16}$$

where n is the slope of the power spectrum, $n(k) = d\log(P(k))/d\log k$. For $n > -3$ the amplitude of fluctuations is larger on small mass scales, so that the first objects to form are small clumps. Larger clumps form via the hierarchical merging of smaller clumps.

The phase-space evolution of an individual mass element in the full non-linear regime can only be be traced using numerical simulations. There are a few remarkably accurate analytical descriptions of the ensemble averaged mass distribution of objects forming via hierarchical buildup. The original Press-Schechter formalism (Press & Schechter 1974) and the more physical justified extended Press-Schechter formalism (Bond et al. 1991) have been successful in predicting the mass functions found in N-body simulations. The description has been further extended to incorporate the influence of environment on the halo mass distribution Bond et al. (1996); Mo & White (1996); Lacey & Cole (1994); Sheth et al. (2001); Sheth & Tormen (2002); Abbas & Sheth (2005).

1.3 Cosmic Web

The previous section dealt with local evolution of the density values, their higher order moments and their hierarchical evolution. These approaches are often very insensitive to the morphology and topology of the density field. We already saw that the Cosmic Web has the appearance of a very anisotropic network. Such a three dimensional network arises naturally within gravitational collapse. If an overdense proto-patch has an initial asymmetry, then gravity will further enhance this anisotropy.

1.3.1 Zel'dovich Approximation

The Zel'dovich approximation (Zel'Dovich 1970) was the first anisotropic analytical approach that showed how the filamentary network of the Cosmic web arises. In essence it is a ballistic approach, particles are displaced in a direction that is assumed to remain valid in time. The position of the particles for each later time step $\mathbf{x}$ are then given in terms of their original particle positions $\mathbf{q}$ and a mapping term

$$\mathbf{x}(a) = \mathbf{q} + \mathbf{\Psi} * D(a). \tag{1.17}$$

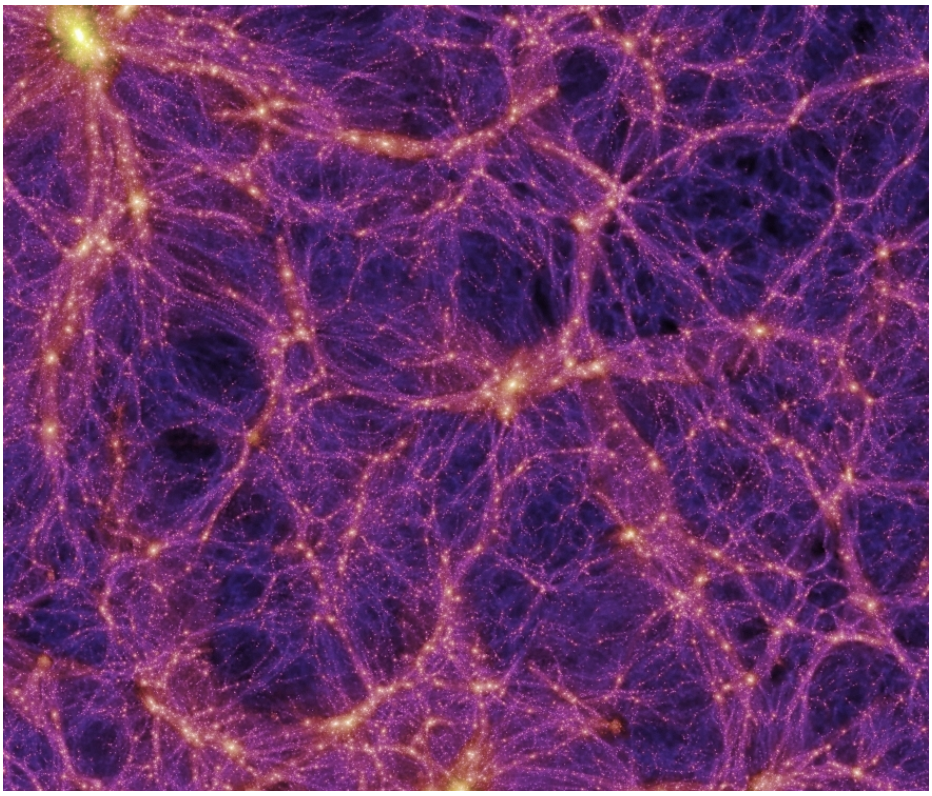

Figure 1.5– Cosmic Web in the Millennium Simulation. The Millennium Simulation is one of the largest dark matter simulation of a concordance model. We can readily identify filaments/walls they connect nodes and resemble strings of pearls. The dark patches show the deep voids, non of these are spherical. Some may appear more triangular, others have a more ellipsoidal shape. Also note the hairlike filaments within the voids, a consequence of the tidal shearing of voids. A strong example can be seen in the larger void on left hand side. From Springel et al. (2005)

Here $D(a)$ is the linear growth factor, $\mathbf{\Psi}$ is the displacement field that depends only on the initial potential field

$$\mathbf{\Psi} \propto \nabla\phi \tag{1.18}$$

The velocities of the particles are also directly proportional to Ψ.

From this mapping we may infer the density, using the fact that the mass within the mapped volume is them same as the mass in the initial volumes

$$\rho d^3\mathbf{x} = \rho_0 d^3\mathbf{q} \quad \rightarrow \quad 1 + \delta = \frac{1}{J} \quad \text{with} \quad J = \left|\frac{\partial \mathbf{x}}{\partial \mathbf{q}}\right| \tag{1.19}$$

J is the Jacobian of the mapping. Using equation 1.17 the Jacobian consists of an identity matrix and another matrix $T_{ij} = \left|\frac{\partial \mathbf{\Psi}}{\partial \mathbf{q}}\right|$, the deformation tensor that is proportional to the initial

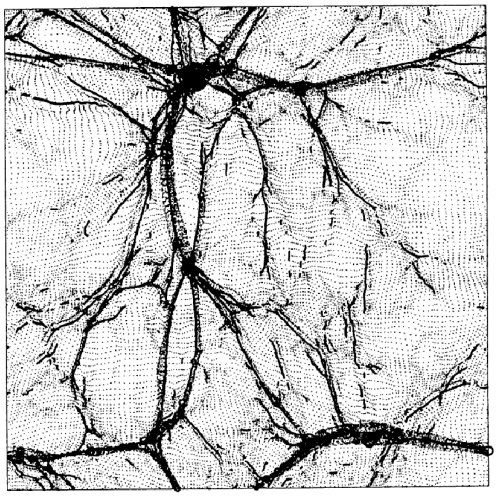

Figure 1.6– Adhesion: The panels illustrates the adhesion approximation. The skeleton of the adhesion model is plotted on top of an N-body simulation with the same initial conditions. When there is not too much power on small scales the adhesion approximation provides a very good approximation of the outline of the Cosmic Web or Skeleton. Image reproduced from Kofman et al. (1992).

tidal field tensor.

$$1 + \delta = \frac{1}{[1 - b(t)\lambda_1][1 - b(t)\lambda_2][1 - b(t)\lambda_3]} \tag{1.20}$$

The $\lambda_1 \leq \lambda_2 \leq \lambda_3$ are the eigenvalues of the matrix T_{ij}. The absolute values of these eigenvalues provide the lengths of the three axes for the local deformation ellipsoid. A positive value means strong compression in that direction, a negative value implies an expansion. Depending on the sign and magnitude of the eigenvalues the formalism provides a natural description of the anisotropic structures in the Cosmic Web. If one (or more) of the eigenvalues is positive this will lead to a collapse in the density field, since the term $1 - b(t)\lambda_1$ will go to 0 for $b(t) \rightarrow 1/\lambda$.

For a Gaussian random field the distribution of the eigenvalues of T_{ij} around the peaks was provided by Doroshkevich (1970) and latter extended by Bardeen et al. (1986). The distribution of the eigenvalues on peak locations can be directly related to the observed collapsed structures. On the basis on the deformation eigenvalues one can distinguish four different morphological components;

Clusters $\lambda_1 \approx \lambda_2 \approx \lambda_3 > 0$
The three axes have the equal compressional value and are also positive. In all direction the collapse is equally strong and this leads to a spherical collapse of the volume.

Filaments $\lambda_1 \approx \lambda_2 > 0$
The largest two eigenvalues are of similar magnitude, while the third is smaller. This will produce a structure collapse in all but one directions, a filament.

Walls $\lambda_1 > 0$
When one of the eigenvalues dominates all the others this leads to a collapse into one dimension, resulting in a two dimensional sheet of matter, or wall.

Voids $\lambda_1 < \lambda_2 < \lambda_3 < 0$
Expansion of the patch in all three direction, this leads to an underdense region $\delta < 0$ or void.

Adhesion approximation

One of the main problems with the Zel'dovich approximation is that particles will always follow a trajectory that is determined by the initial potential field. In reality the orbit will be more complicated. Particles do not follow straight paths to their final haloes, but usually bend into the direction of high density concentrations. Second and higher order Lagrangian perturbation methods may correct the trajectory accordingly.

However, once the particles arrive in a high density object, even with the higher order approximations the particles would still pass through the halo. Eventually, this leads to an evaporation of the structures.

In reality the particles will fall into collapsed objects, and get bound to the emerging virialized halo. In some sense particles 'stick' to the non-linear potential wells. The adhesion approximation (Gurbatov et al. 1989; Shandarin 1991; Kofman et al. 1990) tries to incorporate this process by introducing an artificial viscosity parameter that makes particles stick. In Figure 1.6 we show an example of large scale structure in the adhesion model made by (Kofman et al. 1992). The system of expanding and colliding bubbles in the adhesion model naturally leads to a Voronoi like cellular pattern of the large scale structure (Sahni et al. 1994).

1.3.2 Cosmic Web in CDM

When there is a small scale cut-off (i.e. hot dark matter) the potential is relatively smooth, then the Zel'dovich approximation provides a very accurate description. For a spectrum with a small scale cut-off the first collapsed structures to appear would be large weblike structures. The CDM does not have such a sharp truncation and structures forms in a hierarchical fashion. Bond et al. (1996) showed that also in a CDM scenario such weblike structures would emerge. The same large scale wavelenghts that produce the classical walls and pancakes are still present in the CDM initial conditions. These large scale overdense structures, like clusters, constrain the matter distribution to form linking bridges in between them (see Chapter 5 such bridges). In this case the filaments would not look like the smooth uniform caustics as usually seen in the Zel'dovich and Adhesion approximation. Instead, these filaments are made up of smaller haloes, much like a string of pearls. In this sense they differ from the classical pancakes, since they would not form the caustics in the density field.

The picture that is most relevant is one where there are small collapsed objects that travel along a smooth flow governed by larger structures. The prevalence of the filamentary pattern is very much determined by the slope $n(k)$ of the spectrum. For a flatter spectrum, i.e. $n \rightarrow -3$, the Cosmic Web becomes more pronounced, due to the extra coherence at large scales. The small scales produce local chaotic motions within the regime of the Cosmic Web these can be ignored. The transition from global and smooth flow to local random flows can be associated with transition scale from the linear regime to the full non-linear regime. This approach leads to the peakpatch formalism developed by Bond & Myers (1996); Bond & Myers (1996a,b).

An illustration of how this Peakpatch process forms the Cosmic Web can be seen in Figure 1.7. It shows a thin slice through the initial condition of a Gaussian Random Field. Within this cube the collapsed spheres were hierarchically identified in accordance with the excursion set approach (see section 1.2.4). These spheres are shown in the top-left panel. One immediately sees that these peaks in the Lagrangian space are already strongly clustered Bardeen et al. (1986). Massive peaks cluster more strongly. Even in low density regions the small peaks cluster together. Abbas & Sheth (2007) showed that is a consequence of the clustering of large dips in the primordial density field.

This clustering is further amplified when the peaks are moved to their present day Eulerian position. This is shown in the top-right panel. One may immediately see the outlines of large voids and filaments. This becomes even clearer when we collapse peaks to their Eulerian

size. The coherent flow of collapsed peakpatches forms the outlines of walls and filaments.

The pattern of filaments and walls is directly defined by the presence of the most massive clusters. Their tidal influence constrains the matter and galaxies to reside in filaments that bridge the clusters. The Cosmic Web theory predicts that the strength of the filaments depends on the mass, mutual distance and orientations of the clusters. In other words "clusters weave the Cosmic Web" (Bond et al. 1996).

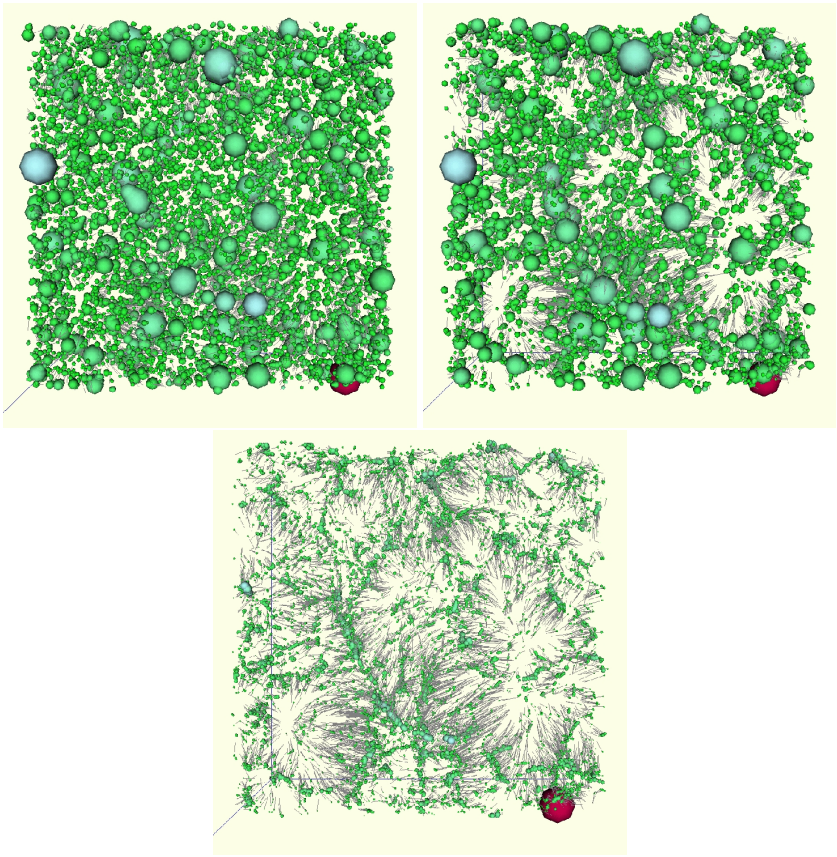

Figure 1.7– Peakpatch Formalism of the Cosmic Web We show the appearance of the Large Scale Structure in a XY slice trough a $200h^{-1}$Mpc box. The top-left panel shows the Hierarchical identified peaks list in the Initial Conditions/Lagrangian coordinates. The top-right panel shows the peakpatches moved to their Eulerian coordinates, as indicated by the grey lines. The bottom panel shows the same patches as the top-right panel, but now shown for spheres with sizes according to the virial radius. Note how the coherent out flows of peaks create large voids, while at the same creates large filaments where such out flow regions collide. See for example around the large filament running in the lower left corner.

1.4 Voids

The one component of the Cosmic Web that receives particular emphasis in this thesis is that of the population of voids. Not only are they a prominent feature of the large scale Universe, but they also appear to contain a considerable amount of information on the global cosmological parameters. Furthermore, they provide a vital testing ground for the understanding of galaxy formation.

1.4.1 Basic Void properties

On the basis of some simple models, like the spherical and ellipsoidal model, we may list the following properties.

- *Voids Expand*.
  The underdensity of a void corresponds to a weaker interior gravitational field. With respect to the global universe this leads to an effective (peculiar) gravity inducing a general flow out of the void region.

- *Voids Empty*.
  As matter streams out of the void, the density within the void decreases. Isolated voids will asymptotically evolve towards an underdensity $\delta = -1$, pure emptiness.

- *Voids form Ridges*.
  As the density within voids gradually increases outward, the corresponding peculiar (outward) gravitational acceleration decreases outward: void matter in the centre moves outward faster than void matter towards the boundary. As a result matter accumulates in ridges surrounding the void (see fig. 1.8). The steepness of the resulting density profile depends on the protovoid depression (Palmer & Voglis 1983).

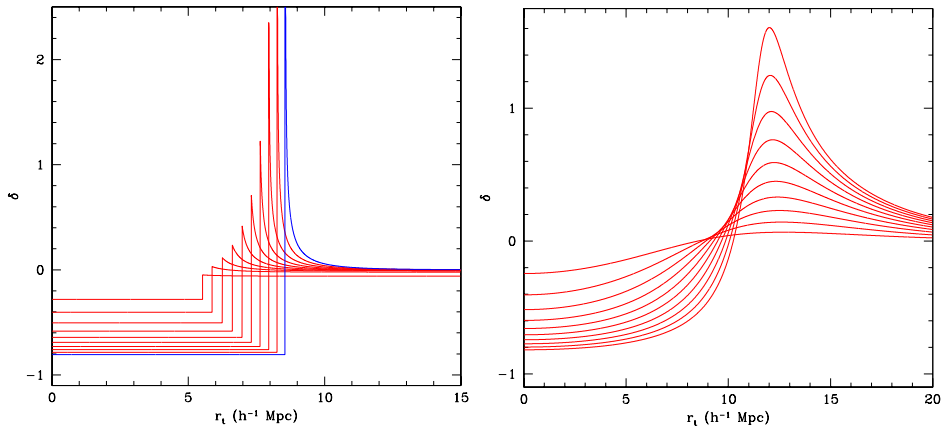

Figure 1.8– Spherical Void The figure show the evolution of an one dimensional void. The left and right figure start with two distinct initial profiles. One may recognise three important characteristics of the void evolution (i) *Voids expand*, (ii) *Voids get more underdense* and (iii) *Void boundary gets overdense*

- *"Bucket" Density Profile*
  Voids assume a "bucket" shape – marked by a uniform interior density depression and a steep outer boundary – as a result of the fast outflow from the "flat" centre in a primordial underdensity. While their matter content accumulates near and around steep density ridges, the interior involves into a region resembling a low-density homogeneous FRW Universe (see fig. 1.8).

- *Superhubble Void Expansion*
  Related to the uniform density interior of mature voids the corresponding peculiar velocity field is that of a "Superhubble" flow (Icke 1984): the interior flowfield of voids is marked by a uniform velocity divergence (Schaap 2007). For a spherically symmetric void model it is rather straightforward to analytically infer that this is the expected natural tendency for voids (see fig. 1.8). It is a manifestation of Birkhoff's theorem, according to which a void region can be described as an isolated lower Ω FRW universe (van de Weygaert & van Kampen 1993; Goldberg & Vogeley 2004).

- *Characteristic Void & Shellcrossing*
  Overdense spherical peaks have a characteristic and time of collapse, coincident with a linearly extrapolated density $\delta_c = 1.69$. Voids have a similar globally valid characteristic epoch of evolution, that of *shellcrossing*. This happens when interior shells of matter take over initially exterior shells. It happens when a primordial density depression attains a linearly extrapolated underdensity $\delta_v = -2.81$ (for EdS universe). A perfectly spherical "bucket" void will have expanded by a factor of 1.72 at shellcrossing, and therefore have evolved into an underdensity of $\sim 20\%$ of the global cosmological density, ie. $\delta = -0.8$.

- *Identity observed voids*
  Bertschinger (1985) demonstrated that once voids have passed the stage of shellcrossing they enter a phase of self-similar expansion. Subsequently, their expansion will slow down with respect to the earlier linear expansion. This impelled Blumenthal et al. (1992) to identify voids in the present-day galaxy distribution with voids that have just reached the stage of shell-crossing.

- *Non-linearity of Voids*
  While by definition voids correspond to density perturbations of at most unity, $|\delta_v| \leq 1$, mature voids in the nonlinear matter distribution do represent *highly nonlinear* features. This may be best understood within the context of Lagrangian perturbation theory (Sahni & Shandarin 1996). Overdense fluctuations may be described as a converging series of higher order perturbations, the equivalent perturbation series is less well behaved for voids. The successive higher order terms of both density deficit and corresponding velocity divergence alternate between negative and positive

1.5 Beyond Isolation

In realistic circumstances voids are never isolated, and their evolution is strongly influenced by their surroundings and internal structure. This is a direct consequence of the mild density deficit in voids, which can never be lower than -1, and their extended nature.

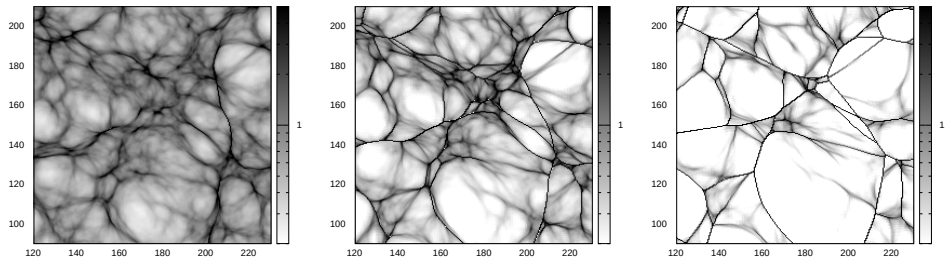

Figure 1.9– Sticky Void Collapse: The figure shows the skeleton of Cosmic Web in the adhesion approximation. Three times slices are shown, at various location in the Cosmic Web one can identify regions where small voids disappear. Especially in the last slice many of the small voids have collapsed along with the nodes and filaments. The images were produced with an efficient geometric adhesion code developed by J. Hidding.

1.5.1 Void Shape

For large voids the evolution toward a spherical profile has been established only for the inner parts of the void (see e.g. Icke 1984; van de Weygaert & van Kampen 1993). For the boundary of the void the evolution to spherical is less likely to hold. Large voids in the density field are never isolated. This is generically true for any feasible cosmological scenario, since voids are expected to be clustered. Specifically this can be understood from the initial Gaussian Random Field Bardeen et al. (1986).

Neighbouring void regions will strongly constrain the expansion of the other voids. If we consider voids as equally expanding bubbles, then the material that streams out of the voids will create walls in between both voids. In a Universe filled with such expanding voids this will produce a cellular pattern of non spherical voids (Icke & Van de Weygaert 1987; Van de Weygaert & Icke 1989; Regos & Geller 1991; Dubinski et al. 1993).

Besides neighbouring voids, large overdense regions also influence the evolution of a void. In fact due to the relatively mild values of the density contrast for voids $-1 < \delta < 0$ the involved accelerations are rather small. The external forces may easily perturb the shape of the void. One may therefore qualitatively understand that the faster growing high density peaks find it easy to distort the shape of voids. The shape of the void should be predominantly determined by the external tidal fields acting upon a void.

Small voids may disappear when a large volume collapses to form an overdense structure. Such smaller voids within the overdense regions will be easily distorted by the anisotropic collapse (van de Weygaert et al. 2004). Before they have completely collapsed the small voids will attain a very non-spherical shape (see also the void collapse illustrated in Figure 1.9).

It is thus very unlikely for non-isolated small *and* large voids to be spherical. The shape of the voids to first order can be predicted by the external Tidal field acting upon a void (see Chapter 3).

1.5.2 Adhesion Voids and the anisotropic Void collapse

The adhesion approximation allows a rigorous study of the evolution of voids within a more generic setting. Sahni et al. (1994) studied the time evolution of the void population. They noticed that for a given scale voids of that size only emerge at a certain time. When these voids appear, at the same time also the filaments and walls form that define these voids. As the new generation of large scale voids matures smaller voids will disappear. They are preferentially

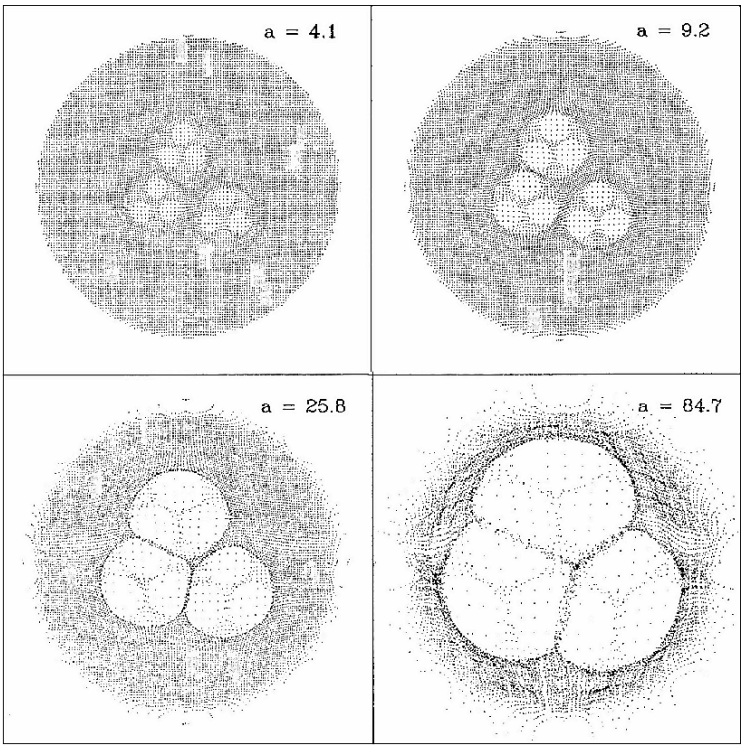

Figure 1.10– Toy model for Voids: The figure shows the evolution of the void hierarchy in an isolated spherical void. Within this void three subvoids are made, which are again split up into three subvoids. In the top-left panel the initial conditions are shown, in the top right panel the figure shows the appearance of nine small voids. They merge into three larger voids visible in the lower left panel. The lower right panel shows the appearance of on large void. The imprint of the previous generation of voids is still visible as the diluted substructure. Form Dubinski et al. (1993)

located around the edges of the new generation of larger voids, therefore they are likely to collapse along with the formation of the larger filaments.

This process is illustrated in Figure 1.9. In three time steps we show the formation of two large voids. As the large voids start to outline their boundary, the smaller voids on it sides collapse along with the formation of the filaments. We may notice that the typical void size becomes larger and that the cellular pattern attains a simpler appearance Sahni et al. (1994).

1.6 Void Hierarchy

In the previous section we considered the influence of voids not being isolated in the density field. Not only neighbouring voids and clusters have to be considered to describe the evolution of underdense regions. One may consider another kind of influence at different scales various proto-void regions may overlap in the initial conditions.

The small scale voids are related to a hierarchical buildup of voids. Like large haloes, large voids are formed from the merging of smaller voids. Small scale voids also merge into larger

void objects. Two small voids may merge when the material that is located in between the void walls will empty out towards the edge of the gradually fading inter-void wall. As this void wall empties out, the voids will merge and form a single larger void.

The previous generation of voids will remain visible as tenuous remnants in the larger voids. The formation of these subvoids is illustrated in Figure 1.10 (Dubinski et al. 1993). It shows a toy model for the formation of void hierarchy via the merging of nine small voids into three larger voids. These three voids merge again into one larger void, while the substructure within the void slowly disappears. Even in the last output slice the nine initial voids are still recognisable.

A similar process can be seen in a large void in N-body simulations. Here we show the evolution of a large void in $100h^{-1}$Mpc box. A constrained random field was generated with a 2σ at a scale $8h^{-1}$Mpc. The void expansion can be clearly seen. The outer edge of the void remains strikingly non spherical. The neighbouring voids and clusters on its edge give the boundary the appearance of almost piecewise linear edges. This also influences the smaller voids on its outer edge. The shape of those smaller voids are oriented parallel to the surface of the void. For small voids located near the edge of the void the expansion of the large void may be strong enough to push the smaller out of existence (van de Weygaert et al. 2004). While the inner parts of the large void evacuate, small remnants remain lingering in the interior.

1.7 The Evolution of the Void population

The hierarchical evolution of haloes can be relatively accurate predicted using spherical or ellipsoidal collapse model. The merging process for voids is more complicated than for the haloes. For voids not only void-merging is relevant, also nearby overdense structures influence the voids. The shape of the voids is directly influenced by the surrounding overdense structures. In fact it can even go further, since smaller voids may collapse along with larger overdense regions. Sheth & van de Weygaert (2004) have worked out the resulting void size/mass distribution. They showed that distribution is marked by peak sized distribution.

The distribution is characterised by a decreasing probability toward large voids, since the very large voids are generated by the rare events in the Gaussian random field. The truncation at small scales is provided by collapsing voids. The smaller the void, the more likely it is to be located in either a larger scale overdense or underdense object. This leads to a truncation of the void distribution at small scales.

In Figure 1.12 shows the void distribution in a $\Omega = 1$ model with a powerlaw power spectrum. When we compare the green curve for no void collapse and the curves that do have a void collapse correction (black and red curves) we see a clear impact on the presence of small scale voids. The resulting peaked void size distribution provides a natural explanation for the cellular appearance of the large scale structure (Einasto et al. 1980; Zeldovich et al. 1982; Van de Weygaert & Icke 1989; Sahni et al. 1994)

1.8 Voids as Cosmological Probes

In principle one would like to use the size distribution of voids as cosmological probe. In similar way as the abundances of large cluster one should be able to use the number of large voids to probe Ω_m and σ_8. There are unfortunately two complications with this approach.

The void distribution is very sensitive to the definition/voidfinding approach, which makes it difficult to compare the measured distribution to the theoretical excursion set void distribution (Sheth & van de Weygaert 2004). Another complicating factor is the sensitivity of the voids sizes to biasing process (Little & Weinberg 1994, see also Chapter 5 and Chapter 7). To make cosmological inferences we have to relate the observed galaxy void to the dark

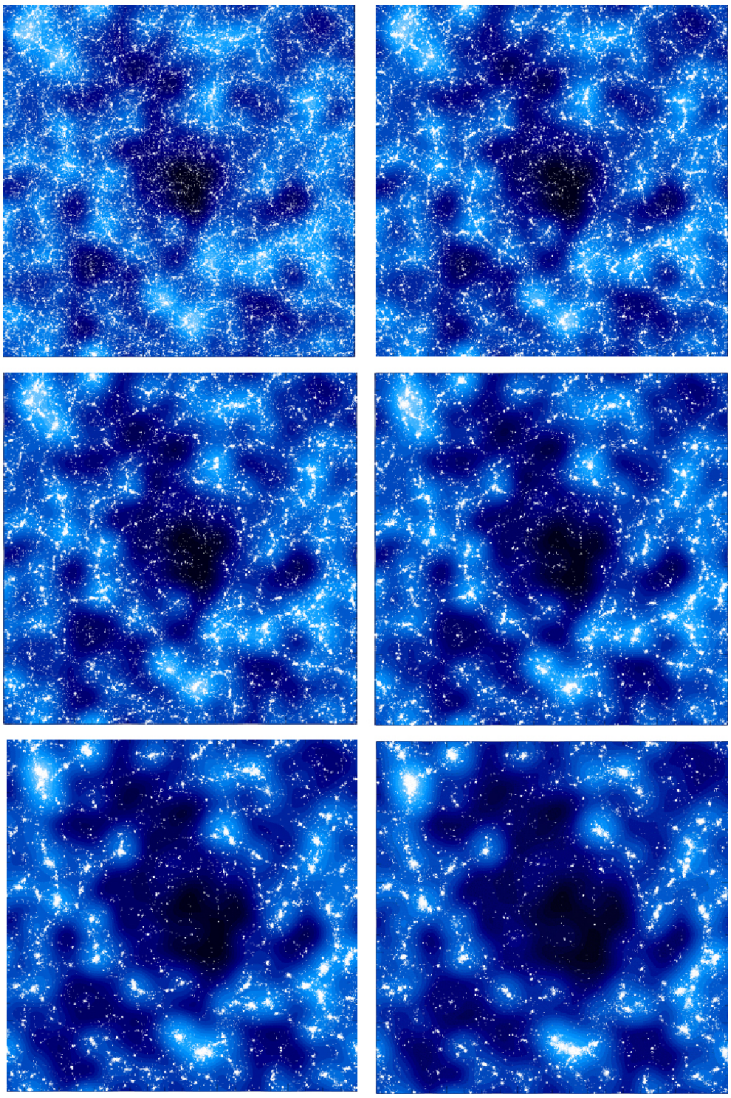

Figure 1.11– General Void Evolution Six time steps in the evolution of a large void in an N-body simulation. On the initial field was imposed a constrained that at $8h^{-1}$Mpc we created a 2σ underdense region. We may recognise how the inner parts of the voids stream empty and we may even see the formation of large overdense structures on its outer edge. These more overdense structures on the edge clearly collapse and form larger overdensities, yet more or less remain fixed at their initial locations. The final voids show still ample substructure within the central region. The large void is surrounded by smaller voids, that seem to be squeezed away by the outward push and pull of the large void and the clusters that surround it.

matter defined voids. The way galaxy defined voids compare to the underlying dark matter may not be straightforward if biasing is complex (Arbabi-Bidgoli & Müller 2002; Furlanetto & Piran 2006).

Betancort-Rijo et al. (2009) suggest to use largest voids ($13h^{-1}$Mpc) where biasing is of lesser importance. This scale roughly corresponds to voids that originate from similar sized perturbations as clusters. Like clusters it provides a probe on σ_8 and the shape parameter of the spectrum $\Gamma = \Omega_m h$. For the very small scale voids, so-called 'mini-voids', biasing becomes very important. This provides another unique probe for testing the ΛCDM galaxy formation scenarios (Tikhonov & Karachentsev 2006). Recently Tikhonov & Klypin (2009) observed that small scale voids (or the void probability function) in the Local Volume ($< 8Mpc$) are consistently too large than expected from a ΛCDM scenario.

Another strong dependence on cosmology can be found in the shapes of voids. To first order the shape of large voids should also be less sensitive to the biasing. Originally the suggestion was that the redshift distortion of voids could be used as a measure of the Ω_m. Assuming that voids are spherical expanding bubbles, the front part of the void would be mapped towards the observer, whereas the backside would be mapped further away. In redshift space, voids would appear extended in the line of sight. The amount of void distortion

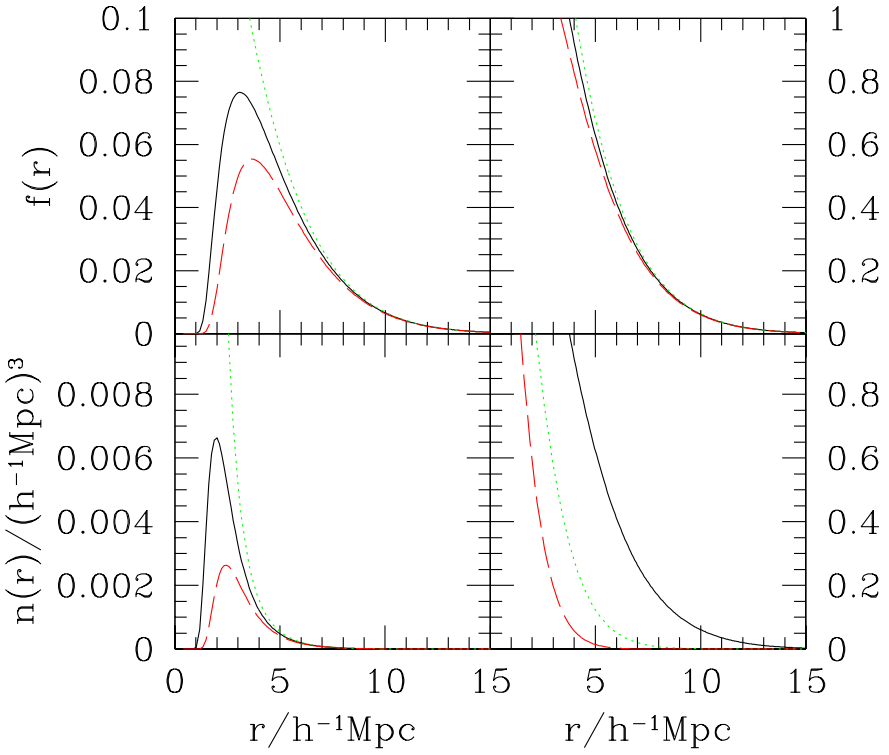

Figure 1.12– Peak Void Size Distribution: The figure shows the size distribution of voids. The green lines represent the void distribution without void collapse corrections. The black and red curve shows the void distribution with the void collapse. The red-curve has a lower collapse threshold than the black curve. From Sheth & van de Weygaert (2004)

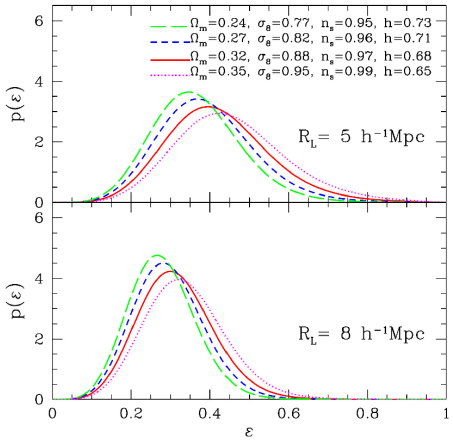

Figure 1.13– Void Shape: The shape of voids is determined by the underlying cosmological parameters. Depending on the parameters at certain scales the voids are more or less ellipsoidal. Image from Park & Lee (2007)

depends on the expansion velocity inside the void. These velocities are directly related to the value of Ω_m and σ_8 via the velocity growth factor, $f(\Omega_m)$ (Peebles 1980; Regos & Geller 1989, 1991; Dekel & Rees 1994; Ryden & Melott 1996; Bernardeau & van de Weygaert 1996). In case of low density Universes $\Omega_m < 1$ this effect is very small, and therefore not of practical use.

Possibly much more interesting is that of the external influence on the intrinsic shape of voids. Because the cosmological parameters entirely specify the power spectrum of initial fluctuations, one may use the void shapes to infer their values. In the full nonlinear regime this shape can be rather complicated (Shandarin et al. 2004). At larger scales, relevant to the galaxy defined voids, we may approximate the tidal forces using the Zel'dovich approximation to infer the void shape (Park & Lee 2007).

Figure 1.9 shows the ellipticity distribution of voids for two different scales. The figure shows that we may not expect voids to be spherical underdense regions. The intrinsic shape is dependent on the underlying cosmology, and therefore it can be used to constrain the cosmological parameters (Park & Lee 2007; Lee & Park 2009; Lavaux & Wandelt 2009). In figure 1.13 the shape distribution of voids is plotted for four ΛCDM like cosmological models. Lee (2009) used this dependence to estimate the normalisation parameter $\sigma_8 \approx 0.9$.

1.9 Matter and Galaxies inside Voids

The pristine low-density environment of voids represents an ideal and pure setting for the study of galaxy formation and the influence of cosmic environment on the formation of galaxies. Voids are in particular interesting following the observation by Peebles that the dearth of low luminosity objects in voids is hard to understand within the ΛCDM cosmology (Peebles 2001).

In the following we will discuss separately the haloes and galaxies populating the voids.

1.9.1 Void Haloes

The abundance of substructure in large voids is reflected in the existence of a population of haloes. Due to the underdense environment the halo mass function is not the same as in more overdense regions. In some sense voids can be sense as low density Universe with a larger Hubble parameter (see Goldberg & Vogeley 2004). This cosmological rescaling has three prominent influences on the haloes that reside in low density regions.

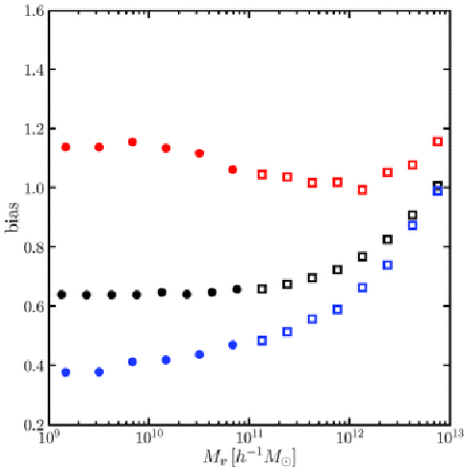

Figure 1.14– Assembly Bias: The figure shows the assembly bias as measured in the Millennium II simulation by Boylan-Kolchin et al. (2009). The clustering strength as function of dark matter mass for the oldest population (red), the youngest (blue). From Boylan-Kolchin et al. (2009)

1. Due to the freeze out of structure growth $z_f = \Omega_m^{-1} - 1$, perturbations have most of their growth at early times (van de Weygaert & van Kampen 1993; Goldberg & Vogeley 2004).

2. The distribution of halo masses in voids shifts to lower masses (Mo & White 1996; Sheth & Tormen 2002; Benson et al. 2003; Friedmann & Piran 2001; Gottlöber et al. 2003; Colberg et al. 2005; Aragón-Calvo 2007, see Figure 1.15 and further below).

3. Haloes of a given mass are younger in voids than in higher density regions, the halo formation bias. Another way of phrasing this, is that a given halo mass at low density has been assembled more recently than the same halo in an overdense environment (Tully et al. 2002; Sheth & Tormen 2004; Gao et al. 2005; Wechsler et al. 2006; Harker et al. 2006; Hahn et al. 2007, see Figure 1.14)

4. The low mass dark matter haloes in the void environment have a lower concentration (Hoffman et al. 1992; Avila-Reese et al. 2005; Wechsler et al. 2006).

5. Void haloes find themselves located in filamentary and sheet like structures. (van de Weygaert & van Kampen 1993; Gottlöber et al. 2003; Sheth & van de Weygaert 2004; Patiri et al. 2006; Park & Lee 2009; Park & Lee 2009). This may even lead to a stronger clustering of the galaxies in the least dense part of the void (Abbas & Sheth 2007).

6. The haloes of a given mass have the lowest spin parameter λ inside voids (Hahn et al. 2007). On the other hand, Aragón-Calvo (2007) found that this effect may disappear dependent on the halo finder.

7. Towards the edge of the void there is a strong alignment of the major axis of the halo with the void surface. The angular momentum also has the tendency to lie parallel to the void-wall (Trujillo et al. 2006; Aragón-Calvo et al. 2007; Brunino et al. 2007; Cuesta et al. 2008; Zhang et al. 2009).

The first and the last points might seem to be at odds with each other. They in fact do not have to be. Even if the growth within voids is small compared to the rest of the Universe, it is not zero. According to the second point the voids are populated with lower masses haloes.

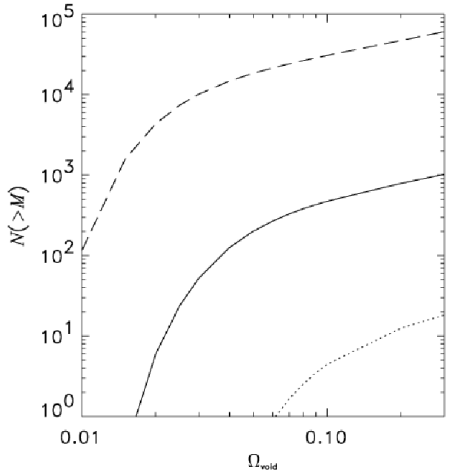

Figure 1.15– Halo mass: The figure show the number of haloes above a certain halo mass as function of the average underdensity within a $10h^{-1}$Mpc Void. The underdensity of the void is expressed as a rescaled Ω_m Universe. Here $\Omega_m = 0.3$ would be a void of average density contrast, the expected void contrast of $\delta = -0.2$ would correspond to a value of $\Omega_m = 0.06$. The three curves show the number of haloes above a limiting mass of respectively $1 \times 10^8 M_\odot$, $1 \times 10^{10} M_\odot$ and $1 \times 10^{12} M_\odot$. Form Gottlöber et al. (2003)

The same low mass haloes in high density regions are subhaloes of larger collapsed structures. Such subhaloes will most likely not grow anymore (see Goldberg et al. 2005; Dalal et al. 2008). Therefore, even the relatively small growth (item 1) for the lower mass void haloes (item 2) can explain the later assembly of void galaxies.

Halo mass in voids

The lowering of the halo mass can be understood if one adjusts the collapse barrier in the excursion set formalism (Bond et al. 1991; Mo & White 1996; Sheth & Tormen 2002). The random walk would not start at zero but at a lower density at some large filter scale. The probability of the random walk then crossing the barrier at some given mass scale decreases with the lowering of the average density inside the void. Effectively we have a higher collapse barrier in low density environments. This is reflected in the void halo mass population that shifts toward smaller halo masses (Friedmann & Piran 2001; Gottlöber et al. 2003). Martino & Sheth (2009) showed that the increase of the barrier is equivalent as regarding the void as a low density Universe of the same age with higher Hubble parameter (Goldberg & Vogeley 2004; Goldberg et al. 2005).

1.10 The properties of Void galaxies

First we shall summarise a few of the most outstanding properties of void galaxies, a summary extracted from a heterogeneous sample of references [*]. After that we shall try to put them in the context of general and global trends of galaxy properties.

1. Void galaxies have lower stellar mass (Croton et al. 2005; Goldberg et al. 2005).
2. Void galaxies are bluer (Grogin & Geller 1999; Rojas et al. 2004; Croton et al. 2005).
3. Void galaxies are hosted by similar mass dark matter haloes as in overdense regions (Goldberg et al. 2005; Hoyle et al. 2005).

[*]As a first order approximation, we assume that void galaxies are galaxies that are isolated, live in underdense regions, or in low clustering environments. Strictly speaking this is not the case: an underdense galaxy may in fact also be located in a wall environment.

4. Stellar population of void galaxies are younger (Grogin & Geller 2000; Kauffmann et al. 2004; Rojas et al. 2005).

5. Galaxies in voids might have a small blue excess (Park et al. 2007; von Benda-Beckmann & Müller 2008).

6. Void galaxies have higher star formation rate (Grogin & Geller 2000; Rojas et al. 2005; González & Padilla 2009).

7. AGN activity is higher in low density environments (Kauffmann et al. 2004; Constantin et al. 2008).

8. Void galaxies are more likely to be of late-type (Dressler 1980; Postman & Geller 1984; Croton et al. 2005; Hoyle et al. 2005).

9. Low mass void galaxy systems may have lower stellar concentration (Kauffmann et al. 2004; Rojas et al. 2005).

10. The cold gas fraction in voids seems to follow the global trend with luminosity (not taking into account cluster environment) Stanonik et al. (2009). (But see Huchtmeier et al. 1997; Pustilnik et al. 2002; Geha et al. 2006; Grossi et al. 2009).

11. Voids do not appear to be populated by a particular kind of galaxy type, such as low surface brightness galaxies, emission line galaxies, gas rich dwarfs or HI clouds/Lymann α absorbers (Dekel & Silk 1986; Weinberg et al. 1991; Stocke et al. 1995; Hoffman et al. 1992; Szomoru et al. 1996; Kuhn et al. 1997; Popescu et al. 1997; Peebles 2001; Stocke et al. 2007).

The environmental influence on galaxy properties has long been established and known as trends with density and galaxy morphology (Dressler 1980). At high density feedback processes like strangulation, quenching, ram pressure stripping, tidal stripping operate that may help to produce a population of on average more red and gas poor galaxies. The high density environment also makes it easier for galaxies to grow fast, and produce massive objects, see section above.

Toward the lowest density we find on average more spiral galaxies that have bluer colours and high star formation rate. They are gas rich and actively forming stars, and have lower average stellar masses. Especially star formation is very dependent on environment. Moving to low density one sees an increase of the star formation rate. Related to the higher star formation is the increase in AGN activity in low density regions.

The question arises what are the main drivers behind these effects. The main result seems to indicate that stellar mass and star formation history control most of the environmental relationship (see Blanton & Moustakas 2009, and references therein). According to Kauffmann et al. (2004); Patiri et al. (2006); Tinker et al. (2008); Tinker & Conroy (2009); Croton & Farrar (2008) such trends in void galaxies are predominantly explained with the decrease of the average halo mass as function of density (item 3 in the void halo properties list). Most present day star formation has shifted to low mass galaxies, so that the trends of higher star formation in voids can be understood from this shift. Accordingly, it is claimed that the other trends, especially those related to star formation activity, can be explained with the decreasing halo mass. Clear examples are the trends in colour (2) and age (4). This would suggest that galaxy formation is relatively insensitive or only weakly sensitive to the other environmental trends. It seems to be most surprisingly insensitive to the assembly bias.

Most of the trends set in at relatively low density. This suggest that local interactions at small scales are most dominant for the evolution of galaxies (Szomoru et al. 1996; Kauffmann

et al. 2004; Park et al. 2007; Park & Choi 2009). This low density can then be explained with haloes becoming subhaloes in the group environment.

The existence of red early type galaxies in voids can most likely be explained by the same formation mechanism as in high dense regions (Croton & Farrar 2008). The AGN feedback may be responsible for the existence of early types, independent of environment. They showed that this produces the observed number density of early types in voids. They also conclude that the properties of these early types should not be dependent on environment. Some tentative claims that suggest otherwise, Schawinski et al. (2007) found that early-types in underdense regions are more active, even after correcting for the fact that one probes lower stellar masses. (However this is still tentative see discussion in section 5.7 in Blanton & Moustakas 2009).

Beyond a density relationship

Concerning low density regions some weak trends have been found that go beyond the relation in just density. Here we shall summarise a few of them

1. Wang et al. (2009) found more isolated red dwarfs in SDSS than expected numbers based on mock galaxy simulations.

2. Park et al. (2007) and von Benda-Beckmann & Müller (2008) found a small blue colour excess in late type void galaxies that goes beyond the dependence on density.

3. Park & Choi (2009) found a weak residual trend with large scale density hinting towards the availability of gas.

4. Schawinski et al. (2009) claim to have found a population of blue early types in underdense regions.

5. Towards the edges of voids Ceccarelli et al. (2008) found an extra increase in the star formation activity

6. The Galaxy Zoo project (Cardamone et al. 2009) noticed there is a population of compact star forming galaxies in low density regions. These are greenish in colour and due to their small size were called green peas.

1.10.1 The Void Phenomenon, is it explained?

The void phenomenon (Peebles 2001) describes the discrepancy between the predicted abundance of dwarf galaxies and the lack of those in observed voids. It also states that the galaxies that are observed in voids do not seem to notice that they live in a fast underdense region. Explanations for the void phenomenon can be roughly divided into those of cosmological origin and those that are related to galaxy formation process

Tinker & Conroy (2009) showed that the void phenomenon can be correctly reproduced in high resolution simulations by assuming a certain relationship between the halo mass and luminosity. Essentially the solution is a steep truncation or suppression of luminosity toward lower mass haloes. It was argued that this relationship can arise from an inefficiency to form stars, possibly due to re-ionisation (Hoeft et al. 2006) and supernova/wind feedback, see Figure 1.16. At the relevant dark matter masses ($10^9 - 10^{10} M_\odot$) there has been no indication that internal processes have removed baryons (Geha et al. 2006; Blanton & Moustakas 2009). Instead, isolated dwarf galaxies seem to be strikingly gas rich. Tikhonov & Klypin (2009); Koposov et al. (2009) noted that the problem for the local neighbourhood can be solved if haloes below $1.0 - 2.0 \times 10^{10} M_\odot$ would not form luminous galaxies. However they found

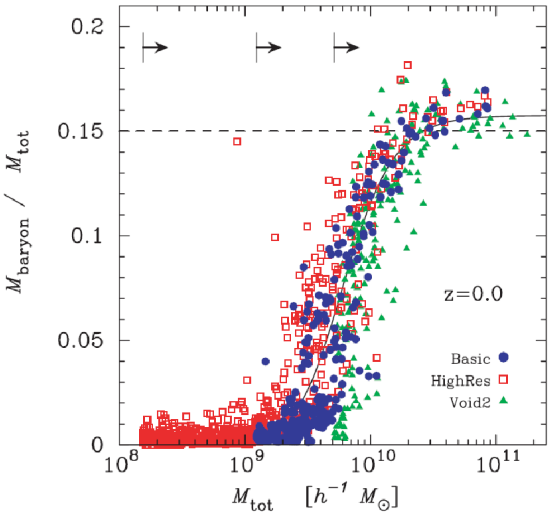

Figure 1.16– Photo-heating: the figure shows the impact of photo-heating on the baryon fraction of low mass haloes. For dark matter haloes below a mass of $10^{10}h^{-1}M_\odot$, the baryon fraction steeply decreases below the Cosmic mean of 0.15.

numerous examples of luminous galaxies with lower dynamical masses. We may conclude they correctly stated that the void phenomenon is not inconsistent with a (strong?) low mass anti-biased ΛCDM model, but incorrectly stated that it was explained. The Tinker & Conroy (2009) model can be tested by determining the mass to light ratio for the observed void dwarfs (Blanton et al. 2008; Tikhonov & Klypin 2009; Stanonik et al. 2009)

1.10.2 The Void Future

The void environment is relatively simple. This may enable it to help break the degeneracy between cosmological parameters and galaxy formation. It is a ideal test for both cosmology as well as the process of galaxy formation. There has been some attention to properties of void galaxies, most of these involve the average properties, like mass, colour, etc. Questions about more specific properties have never been addressed in much detail; Considering their average later build up and lower external tidal forces, where do they attain their angular momentum from (Lee & Lee 2008)? How much material should void galaxies still be accreting at present time? What is the present day merger rate in voids? What happens when a void galaxy arrives from an underdense region into a more overdense region like a wall or filament (Ceccarelli et al. 2008)? Are the star formation rates in void galaxies in agreement with the expected amount of cold accretion (Kereš et al. 2005; Dekel & Birnboim 2006)?

The low mass and low density of void galaxies requires deep and large survey. With the advent of large surveys like the 2dFGRS and SDSS proper samples of void galaxies can be constructed. Also simulations now attain enough dynamic range and sufficient mass resolution to address these questions. In voids it is more straightforward to identify haloes with galaxies, making it more easy to compare simulations to observations. This may provide a strong test case for the *ΛCDM* biased galaxy formation scenario.

1.11 Structure Identification

To address the questions above we need to be able to identify the structures in the matter and galaxy distribution in an objective and well defined manner. In this thesis we discuss and

present new methods to trace the voids, filament and walls in the density field.

1.11.1 Void Definition

For the study of voids a difficulty arises, because there is no proper definition of a void. This can be contrasted to haloes, they will more or less detach themselves from their background and become a virialized object. Virialization is a well-defined dynamical state, no such clear equilibrium definition exists for voids. One possibility for defining voids is at the transition when they go non-linear. At the moment of shell-crossing an initial tophat shaped void has expanded a factor 1.7 and reached a density contrast value of $\delta = -0.8$.

These numerical values may seem useful for defining voids. A complication arises because voids are not spherical. For voids the external influence may be more important than the internal dynamics. This is particular true for void collapse, and the externally determined void shape discussed above. Also, the underdensity criterion used by some methods refers specifically to the internal density of the void. However, such a density value becomes meaningless if the edge of the void is not properly taken into account.

To summarise, the status and the definition of voids still remains very much unclear. To agree upon such a definition, a more extensive effort is needed to let the theoretical void size distributions agree with the measured ones.

1.11.2 Void Finding

A plethora of void finding algorithms has been developed. Each of these methods aims to recover more or less convex underdense regions, yet they differ in numerous ways. The first distinction is that some are aimed for the galaxy distribution, whereas other methods work on the (dark matter) density field.

Another prominent distinction is that some methods are based on void finding using a single isolated sphere or ellipsoid, while other, more advanced, methods use a combination of overlapping spheres or cubes. One class of voidfinders is based on region growing independent of such geometrical primitives. These methods often work on the density field itself. A well known example of such a method is the void defined by the enclosed volume of an iso-density contour Shandarin et al. (2004).

A third class of Void finding methods involves a dynamical reconstruction of the underlying density field. These tend to use second order derivatives (Hessian) of the potential Field (tidal field) or the density field. Void regions are classified as connected Regions according to the signatures of the eigenvalues.

In table 1 we provide an overview of the most commonly used void identification methods. In the Aspen-Amsterdam Void comparison project (Colberg et al. 2008) an initial attempt was made to compare the different VoidFinders. Due to the wildly differing approaches quantitative comparisons are difficult. One can not compare voidshapes for methods based on a single sphere. Another example is the void density. For some methods the density is a parameter that has to be specified. In these cases it does not make sense to compare densities computed with different methods.

To explore how much the method would differ at all, the test was carried out as simple as possible. Within the Millennium simulation the most underdense region was extracted. Located in this subcube is one well defined large void.

Figure 1.17 provides a compilation of the outlines of the void found by different methods. Some strong differences can be seen, they mostly arise from the use of either the dark matter or the galaxy distribution to define voids. Overall the density and size of the voids are most strongly dependent on the void finder.

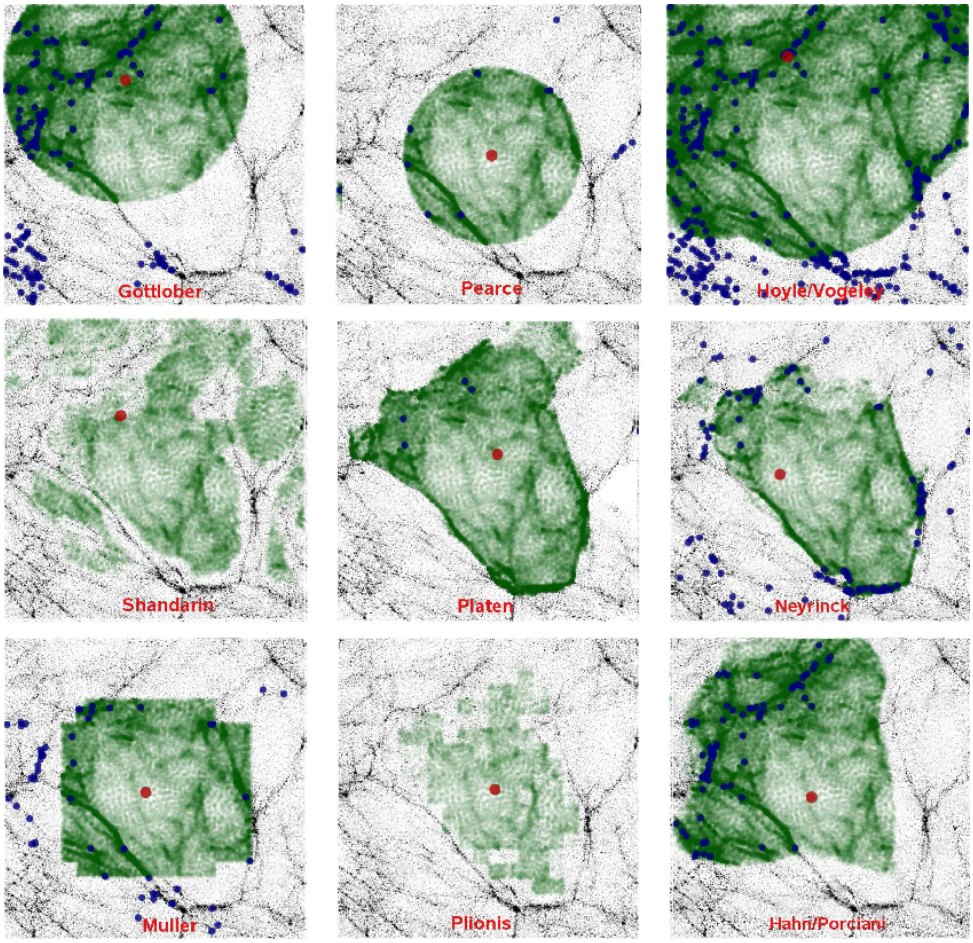

Figure 1.17– Void Finders: we show a compilation of a void found by several different methods. An overview of the characteristics of these methods can be found in table 1. The figure shows the dark matter that belong to each region identified with each method. The red point gives the centre for each void method. The blue dots give a location of galaxies located within the voids. From Colberg et al. (2008)

Besides the differences there are also agreements. Most voidfinders agree that there is a centrally located underdense volume, which is extended along the diagonal that runs from the top left to the bottom right corner. The methods that show this particular volume, differ mostly in the location of the edge of the void. Interestingly the VOBOZ and WVF method agree quite good on the location of the void edge, they both put them at the same high density regions.

The best way to understand most voidfinder is by a growth process that starts from an pre-identified void seed location. From this core the identified void grows outward to the edge of the voids. Take for example the most widely used approach, the sphere growing method. Here consecutively smaller sphere are added to a larger initial seed sphere so to

refine the edge of the void. This method is prone to predefined parameters (linking lengths, overlapping ratio's, etc.). A more natural way is to apply the growth process on the density field itself.

1.11.3 Watershed Void Finder

The Watershed Void Finder, presented in Chapter 2 (Platen et al. 2007), was developed with the aim to provide proper care of the edge of the voids. The idea of the method is that voids are defined by one deep minimum. These can be seen as the starting point for the void growing process. Then we expand the void by steadily adding connected void volumes to the minima. This is done according to the density values, where we start with the smallest density values. This allows us to find voids independent from predefined geometrical objects like spheres or cubes.

One may regard the growth of the voidpatches as the shock front in a flooding or fires. When two of these shock fronts from different minima meet the flood is locally stopped. At these places a segmentation or divide line is drawn, that signals the boundary between two voids. These shock front collisions will first happen at the saddle points in the density field. In fact the segmentation line will start to grow as well along the ridge of the density field. This procedure guarantees that the boundary between two voids will lie exactly on the walls that separate them. In Chapter 4 we have exploited this fact to extract the filaments and walls out of these void boundaries.

1.12 This Thesis

In this thesis we first introduce in Chapter 2 a new void finding algorithm. It is based on the Watershed Transform that facilitates a topological description of the density field by the analogy of a flooding procedure. Within this flooding description the boundaries between the void patches are naturally put on top of walls that separate two voids. The method does not depend on any predefined shape and it is therefore ideal to study the shape of voids in the Cosmic Web.

In Chapter 3 we have analysed the shape of the voids. Here we have look at their mutual alignment. By analysing the marked correlation of the shape tensor. We show that void shape are very strongly aligned over large distances. This effect goes further than a natural alignment of void neighbours. This we have shown by correlating the voidshape both locally with the Tidal Field at various smoothing scales as well as over larger distances at a various smoothing scales. The voids align themselves within the Cosmic Web according to the external large scale Tidal Field.

In Chapter 4 we explore another benefit of the WVF, its ability to detect the natural boundaries Voids; the Cosmic Web. First we will relate the Watershed transform to a more rigorous mathematical background, which is Morse Theory. We develop the Cosmic Spine formalism with which we can find the walls and filaments in the Cosmic Web.

One of the main goals will be to use the Void Finder and Cosmic Spine on observed redshift samples. The watershed transform works on density fields or one any connected lattice with density values. To be able to use the WVF and the Cosmic Spine on observed samples we will first have to investigate qualitatively and quantitatively the reconstruction of density field on observed and mock redshift samples.

In Chapter 5 we investigate what the main sources of errors are in the density field. We have done this by using three different reconstruction methods, one is the DTFE method and a related higher order method called NNFE. These are local methods, we also explore the use of global reconstruction method. Within the global method we saw the appearance of errors that arise because of the sharp extreme high density peaks. Such nonlinear features should not be

Table 1.1– An overview of void finding methods

Method	Input	Intrinsic scale	Idea	Geometry	References
Aiko/Mähonnen	Galaxies	yes - linking length	Climbing the distance field	fine mesh	Aikio & Maehoenen (1998)
Brunino	Halos	yes - seed sphere radius	Underdense + overlapping around lowest density sphere	spheres	Brunino et al. (2007)
Colberg	Density field	yes - minimum void scale	Underdense + overlapping spheres around density minima	spheres	Colberg et al. (2005)
VoidFinder El-Ad/Piran	Galaxies	yes - linking length	Empty + overlapping Spheres in a Wall-Field Galaxy separation	spheres	El-Ad & Piran (1997)
Fairall	Galaxies	yes - integration depth	Visually identified Empty regions	none	Kauffmann & Fairall (1991)
Foster/Nelson	Galaxies	yes - minimum sphere scale	Empty + overlapping Spheres in a Wall-Field Galaxy separation	spheres	Foster & Nelson (2009)
Gottlöber	Halos/Galaxies	no	Spherical empty regions in point set	spheres	Gottlöber et al. (2003)
Hahn/Porciani	Density field	yes - filter scale	Tidal instability in smoothed density field	fine mesh	Hahn et al. (2007)
Hoyle/Vogeley	Galaxies	yes - linking length	Empty + overlapping Spheres in a Wall-Field Galaxy separation	spheres	Hoyle & Vogeley (2002)
Müller	Halos/Galaxies	yes - cube size	Cube growing from maximal low density cubes	cubes	Arbabi-Bidgoli & Müller (2002)
Neyrinck	Density field	no	Region growing from density minima	natural mesh	VOBOZ, Neyrinck (2008)
Pearce	Particles	no	Underdense sphere around minimum density particle	sphere	Brunino et al. (2007)
Platen/Weygaert	Density field	no/yes - filter scale	Region growing from density minima	fine mesh	WVF Platen et al. (2008)
Plionis/Basilakos	Density field	yes - cube scale	Connected underdense cells	cubes	Plionis & Basilakos (2002)
Shandarin/Feldman	Density field	yes - filter scale	Connected underdense regions below isodensity	fine mesh	Shandarin et al. (2004)

interpolated globally, since they represent detached objects from the local trend. However the correct reconstruction of those objects is instrumental to get the correct global smooth density field. The DTFE was shown to be most local and robust against such non-linearities. This we subsequently used in the following Chapters to analyse qualitatively and quantitatively the SDSS reconstructed density field.

In Chapter 6 we provide a cosmographical description of the reconstructed SDSS density field. We will explore the density field slices with increasing distance and discuss the most prominent features in the cosmological density field. Here we have also compared with existing catalogues of LSS objects, like clusters, superclusters and supervoids. This provides us with an illustration of the organisation of the Cosmic Web in Large Wall structures made up of several Superclusters. These are interconnected by cluster filaments that surround huge empty regions, the supervoids. The Boötes Supervoid is the most prominent and outstanding example in SDSS. The SDSS provides is with a beautiful impression of the tessellated large scale structures

A quantitative analysis of the SDSS reconstructed density field is given in Chapter 7. We have put the density field both in the context of cosmology as well as from the galaxy formation point of view. The cosmological aspect is the density distribution of the dark matter. However, we observe the galaxy density field, it is distorted by redshift space distortions and the process of galaxy formation. The latter is often captured in the concept of biasing, the describes the ratio between the dark matter and galaxy density field. Using the Millennium simulation and semi-analytical galaxy formation models as a reference, the probability density function is explored in this Chapter.

Finally in Chapter 8 we present the HI observation of a peculiar void-galaxy. At first sight it might seem unrelated with previous Chapters, but in fact it touches upon all the aspects dealt with in the previous Chapters. Using the SDSS reconstructed density field we were able to select galaxies that reside in deep underdense regions. It is one of the first results of a larger HI void-galaxy project, and entails one of the most peculiar galaxies in the sample. This small void galaxy has a large extended HI-disk, that is oriented perpendicular to the stellar disk. This configuration can be understood if we fold in the fact that this void galaxy resides almost in the centre of a thin sheet in between two large voids. It is isolated, the nearest neighbour galaxy is almost $4h^{-1}$Mpc away. The situation is highly suggestive to cold gas falling in on the void wall and the void galaxy.